Search for Exotic States at $J/\psi \to \rho^0\eta\pi^0$ Based on BESI Data

Ning Wu[1], **Tu-Nan Ruan**[2]

Institute of High Energy Physics, Beijing, 100039[1]
Dept. of Modern Phys, USTC, Hefei, Anhui 230026[2]

June 7, 2000

I. Motivation

♣ Exotic Quantum Numbers:

It is well known that ordinary mesons and baryons are made from quarks. The quark content of ordinary mesons is $q\bar{q}$. According to Quantum Field Theory, the J^{PC} quantum numbers of ordinary $q\bar{q}$ mesons can not be:

$$0^{+-}, 0^{--}, 1^{-+}, 2^{+-}, 3^{-+}, \cdots.$$

These quantum numbers are called exotic quantum numbers.

♣ Exotic States:

According to QCD theory, there is very strong Non-Abel coupling between quark and gluon, and there is self coupling between gluon and gluon. So, some phenomenological models predict the existence of hybrids ($q\bar{q}g$), glueballs(gg or ggg) and four-quark states($qq\bar{q}\bar{q}$). These new states of matter can have exotic quantum numbers. If a meson has exotic quantum number, it is usually called **exotic meson or exotic state**.

♣ Search For Exotic States:

Searching for the evidence of the existence of exotic states is important to both theory and experiments. Recently, E852 experiment at BNL has found some evidences of the existence of exotic states at $\pi^- p$ collisions. The J^{PC}s of these exotic states are 1^{-+}. But the masses of these states are much lower than the expected values given by lattice and some phenomenological models. Besides, their results are not confirmed by other experimental groups after they publish their results. It is important to confirm their results at other experiments.

♣ Search For Exotic States at BES:

According to theoretical estimation, we know that

$$\Gamma(J/\psi \to MH) > \Gamma(J/\psi \to MM') > \Gamma(J/\psi \to MG),$$

where M stands for ordinary $q\bar{q}$ mesons, G stands for glueballs and H stands for hybrids. It means that the J/ψ hadronic decays to hybrid states will have relatively large branching ratios. So the J/ψ hadronic decay is an ideal place for us to study hybrid states and to search for exotic states. BESI has got 7.8M J/ψ events and BESII will got 50M J/ψ events. This provides us a good chance to search for exotic states at BES. Our work is based on BESI and BESII J/ψ data to search for Isovector exotic states through J/ψ hadronic decays.

♣ PWA Analysis on $J/\psi \to \rho^0\eta\pi^0$:

$J/\psi \to \rho^0\eta\pi^0$ is a hadronic decay channel of J/ψ. We supposed that it is accomplished through the following sequential decays:

$$\begin{array}{l} J/\psi \to \rho^0 \quad + \quad X \\ \qquad\qquad\qquad\quad \hookrightarrow \eta \quad + \quad \pi^0. \end{array}$$

Because spatial parity and charge parity are conserved in strong interaction, the J^{PC} of resonance X can only be

$$0^{++}, 1^{-+}, 2^{++}, 3^{-+}, etc.$$

So, this channel is an ideal place for us to search for exotic states by studying the invariant mass spectrum of $\eta\pi^0$ in this channel, and if we find a state whcih has spin 1 or spin 3, it must be a exotic state. This is the advantage of this channel to search for exotic states. We use PWA analysis to study the structure of the mass spectrum of $\eta\pi^0$.

II. Data Selection

We select events which have final state particles $\eta\pi^0\pi^+\pi^-$.

♣ Initial Cut Conditions:

1. Charged Track Selection Criteria

   1) Two charged tracks with zero net charge, $N_{chrg} = 2, \quad \sum Q = 0.$
   2) Good helix fit for MDC tracks, MFIT = 2 or -19.
   3) Polar angle of each track in MDC $|cos\theta| < 0.8$.
   4) Event vertex: $\sqrt{x_0^2 + y_0^2} \leq 2\ cm$; $\mid z_0 \mid \leq 20cm$.
   5) Transverse momentum $P_{xy} > 60Mev/c$.

6) Angle between two charged tracks is less than 175°.
7) Neither charged track deposits more than 0.6 *Gev* of energy in the shower counters; this suppresses radiative Bhabha events.

2. Photon Selection Criteria

   1) Hit in BSC and $Layers > 1$.
   2) $E_\gamma > 70$ MeV.
   3) Shower starts before layer 6.
   4) Angle between the cluster entering and going through BSC should be less than 30°.
   5) Angle between neutral tracks and charged tracks should be larger than 10°.
   6) At least four good photon.

3. Kinematical fit. All surviving events are submitted to the $\gamma\gamma\gamma\gamma\pi^+\pi^-$ $4C$ kinematic fit, $\gamma\gamma\gamma\gamma K^+K^-$ $4C$ kinematic fit and $\eta\pi^0\pi^+\pi^-$ $6C$ kinematic fit. In the initial data selection, it is required that $\chi^2_{4C}(J/\psi \to 4\gamma\pi^+\pi^-) \leq 50$.

♣ Final Cut Conditions:

1)$\chi^2_{4C}(J/\psi \to 4\gamma\pi^+\pi^-) \leq 20$, $\chi^2_{6C}(J/\psi \to \eta\pi^0\pi^+\pi^-) \leq 20$.
2) If we denote the two photons from η as γ_1 and γ_2, and the two photons from π^0 as γ_3 and γ_4. We remove all events which satisfy: $|M_{\gamma_1\gamma_3} - 0.135| < 0.05$, $|M_{\gamma_2\gamma_4} - 0.135| < 0.05$; and $|M_{\gamma_1\gamma_4} - 0.135| < 0.05$, $|M_{\gamma_2\gamma_3} - 0.135| < 0.05$. This removes events of $J/\psi \to \pi^0\pi^0\pi^+\pi^-$.
3) $\chi^2_{4C}(J/\psi \to 4\gamma\pi^+\pi^-) < \chi^2_{4C}(J/\psi \to 4\gamma K^+K^-)$. This removes events come from K^+K^- + neutral tracks.
4) If the momentum of a particle is less than 600 Mev, the particle should be identified to be a π by TOF. $TOF(\pi) > TOF(K)$, if p $<$ 600 Mev.
5) In order to reduce events which come from $J/\psi \to \omega\eta$, we require that $|M_{\pi^+\pi^-\pi^0} - 0.782| > 0.05$ Gev.
6) Define $\Delta^0 = \text{abs}(M_{\pi^+\pi^-} - 0.770)$ $\Delta^+ = \text{abs}(M_{\pi^+\pi^0} - 0.770)$ $\Delta^- = \text{abs}(M_{\pi^-\pi^0} - 0.770)$. We require that $\Delta^0 < \Delta^+$ *and* $\Delta^0 < \Delta^-$.
7) Finally, we require that two charged πs come from ρ decays: $|M_{\pi^+\pi^-} - 0.770| < 0.15$ Gev.

After all these cut conditions, the invariant mass spectrum of $\eta\pi^0$ is shown in Fig. 1. Besides, the ρ^0, η and π^0 signals are shown in Fig. 1 — 2. According PDG, the main background of this channel is $J/\psi \to \omega\eta'$, $\omega \to \gamma\pi^0$, $\eta' \to \eta\pi^+\pi^-$; $J/\psi \to \omega\pi^0$, $\omega \to \pi^0\pi^+\pi^-$; $J/\psi \to \omega\pi^+\pi^-$, $\omega \to \gamma\pi^0$; $J/\psi \to \omega K^\star(892)\bar{K}$, $\omega \to \gamma\pi^0$, $K^\star(892) \to K\pi^0$; $J/\psi \to \omega\pi^0\pi^0$, $\omega \to \pi^0\pi^+\pi^-$; According to our Monte Carlo simulation, We generate 10,000 events and almost no events has gone through all the above cut conditions.

III. Analysis Method

We first write out the covariant helicity coupling amplitudes which describe the following sequential decays:

$$J/\psi \to \rho + X$$

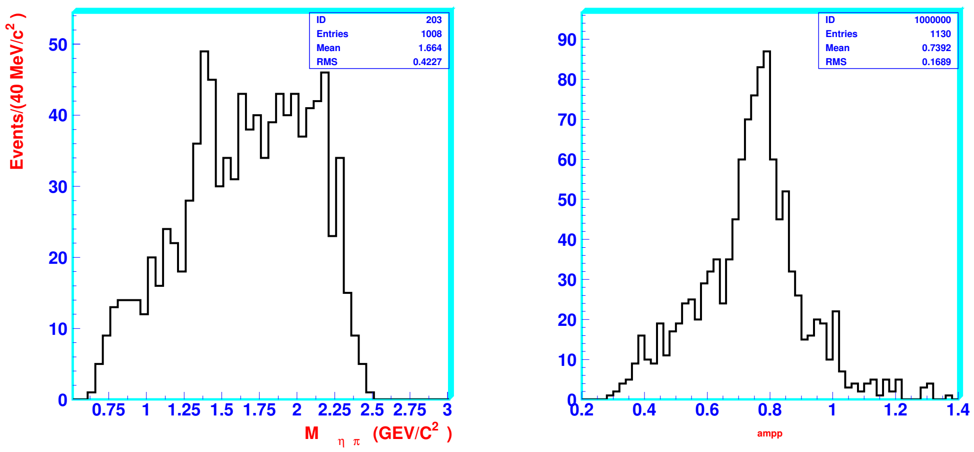

Figure 1: Left: The $\eta\pi^0$ invariant masses spectrum after final cuts; Right: The ρ^0 signal.

$$\rho \to \pi^+\pi^-$$
$$X \to \eta + \pi^0,$$

where resonance X has definite J^{PC}. Then we write out the total differential cross section which describes the whole decay process:

$$\frac{\mathrm{d}\sigma}{\mathrm{d}\Phi} = |A(0^{++}) + A(1^{-+}) + A(2^{++})$$
$$+ A(3^{-+}) + A(4^{++}) + \cdots|^2 + BG,$$

where $A(J^{PC})$ is the total amplitude for all resonances whose spin-parity are J^{PC}. For definite J^{PC}, if N resonances $X_1, X_2, \cdots, X_N$ are added into our solution, the

$$A(J^{PC}) = A(X_1) + A(X_2) + \cdots + A(X_N),$$

where $A(X_i)$ is the covariant helicity amplitude which describes the following decay process:

$$J/\psi \to \rho + X_i(J^{PC})$$
$$\rho \to \pi^+\pi^-$$
$$X_i(J^{PC}) \to \eta + \pi^0.$$

The expression for $A(X_i)$ is:

$$A(X_i) = M^1_{1\ J} \cdot BW(s, m_X, \Gamma_X) \cdot M^1_{00} \cdot BW(s, m_\rho, \Gamma_\rho) \cdot M^1_{00}.$$

Notation $M^{S_a}_{\lambda_b\lambda_c}$ is the amplitude for two body decay:

$$a \quad \to \quad b \quad + \quad c$$

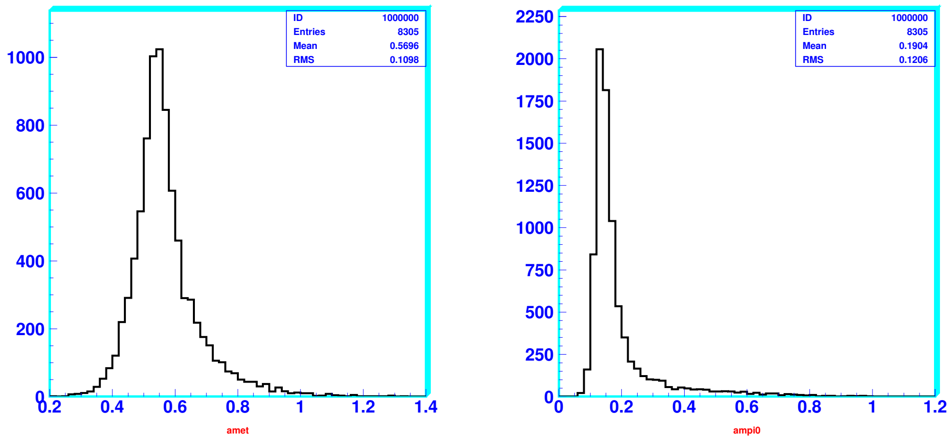

Figure 2: The η, π^0 signals.

$$S_a^{\eta_a} \quad \to \quad S_b^{\eta_b} \quad + \quad S_c^{\eta_c};$$

it is

$$M^{S_a}_{\lambda_b \lambda_c} \sim F^{S_a}_{\lambda_b \lambda_c} \cdot D^{S_a}_{\lambda_a(\lambda_b - \lambda_c)}.$$

The explicit expression for helicity amplitudes $F^{S_a}_{\lambda_b \lambda_c}$ can be found in literature.

Maximum Likelihood Method is utilized in the fitting. The probability density function $f(x, \alpha)$ that describe the data sample is:

$$f(x, \alpha) = \frac{d\sigma}{d\Phi}/\sigma$$

where x is a set of quantities that had been measured by experiment, such as 4-momenta of final state particles, α is a set of unknown parameters which needs to be determined in the fitting and σ is the total cross section of this process:

$$\sigma = \int \frac{d\sigma}{d\Phi} d\Phi.$$

It is given by Monte Carlo integration in the fitting:

$$\begin{aligned} \sigma &= \int \tfrac{d\sigma}{d\Phi} d\Phi \\ &= \frac{\sum_{i=1}^{N_{mc}} \left(\sum_M |A(0^{++}) + A(1^{-+}) + A(2^{++}) + \cdots|^2 + BG \right)}{N_{mc}}, \end{aligned}$$

where N_{mc} is the number of Monte Carlo events. The likelihood function $\mathcal{L}$ is given by the joint probability density of all experimental data:

$$\mathcal{L} = \prod_{i=1}^{N_{event}} f(x, \alpha).$$

In the Maximum Likelihood Method, the central task is to find the maximum of the likelihood function $\mathcal{L}$ by adjusting parameters α. If we define:

$$S = -\ln\mathcal{L},$$

then, finding the maximum of the likelihood function $\mathcal{L}$ will become finding the minimum of S. So, in the data fitting, the task is to find minimum of S by adjusting parameters α.

IV. PWA Analysis and Results

From the mass spectrum of $\eta\pi^0$, we could clearly see the peak of $a_2(1320)$. Besides, there are peaks at about 1690 Mev, 1900 Mev and 2200 Mev, and something exists at the lower mass region.

First, we separate the whole mass region into 6 "bin"s. In each bin, we use our program to fit the angular distributions without adding any Breit-Wigner structure into it. This will tell us that, in each mass region, how many events is 0^{++}, how many is 1^{-+}, $\cdots$. Our results is listed in the Table I.

Mass Region (Gev)	0^{++}	1^{-+}	2^{++}	3^{-+}	4^{++}
0.0 — 1.0	~ 38	~ 8	~ 7	—	—
1.0 — 1.25	~ 26	~ 42	~ 4	—	—
1.25 — 1.5	~ 39	~ 83	~ 36	—	—
1.5 — 1.8	~ 48	~ 25	~ 52	—	—
1.8 — 2.0	~ 7	~ 19	~ 22	~ 16	~ 20
2.0 — 2.8	~ 21	~ 24	~ 23	~ 12	~ 21

Table 1: Event Numbers of various J^{PC}

Now, let's turn to the mass region around 1.4 Gev. According to our bin results, there are both 0^{++}, 1^{-+} and 2^{++} events. According to PDG, there may appear $a_2(1320)$, $a_0(1450)$ and $\rho_1(1390)$. We use these solutions to fit this region and find that all of them are needed for a good fitting here. We have performed mass and width scan on these resonance and obtain their mass and width from these scans. (Fig.3 — 5) We also test statistical significance of these resonances. Our result is listed in Table II. If we change the J^{PC} of $\rho_1(1390)$ to 0^{++} or 2^{++}, the log likelihood will become worse. The related results are listed in Table III. So, our preliminary results favor a 1^{-+} at about 1.39 Gev. And the mass and width on this resonance are close to those results obtained by E852 at BNL.

According to bin results, there are 0^{++}, 1^{-+} and 2^{++} events in the mass region between 1.5 Gev and 1.8 Gev. So we use a 0^{++} or 1^{-+} or 2^{++} to scan this region, we find that only 1^{-+} and 2^{++} have minimum at this region. From these scan results, it seems that 0^{++} events at this region may come from the higher tail of $a_0(1450)$. Our scan results on $\rho_1(1583)$ and $a_2(1670)$ is shown in Fig. 6 — 7.

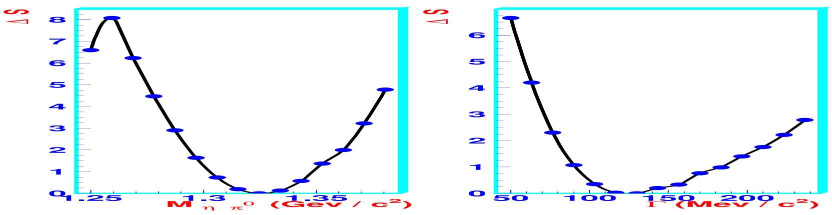

Figure 3: Mass and width scan on $a2(1320)$

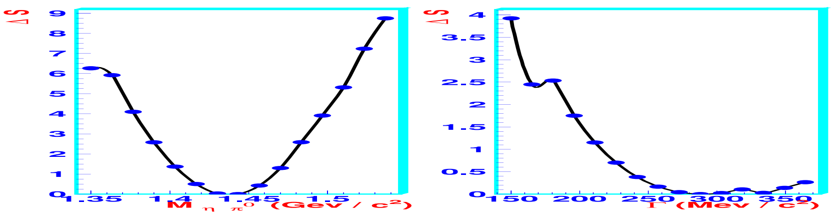

Figure 4: Mass and width scan on $a_0(1450)$

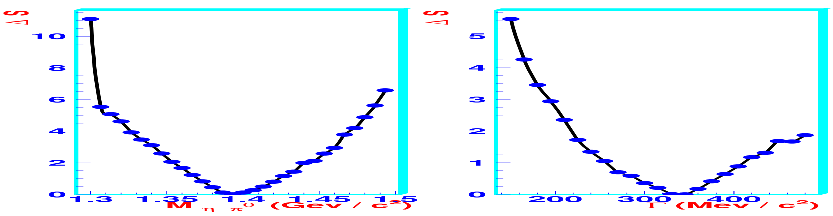

Figure 5: Mass and width scan on $\rho_1(1390)$

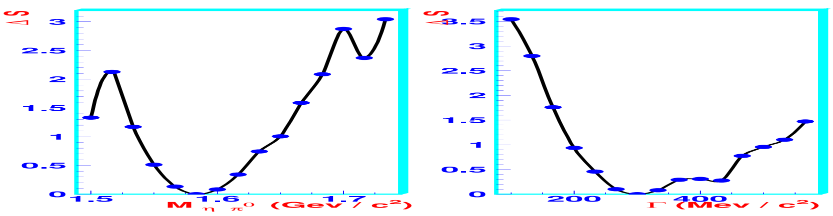

Figure 6: Mass and width scan on $\rho_1(1583)$

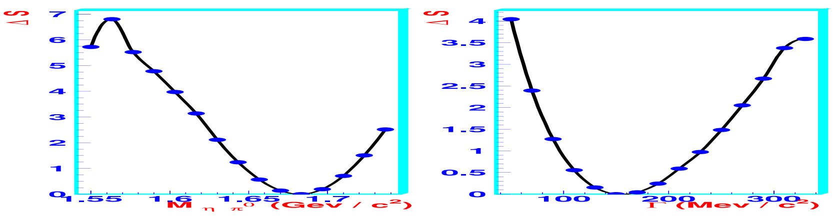

Figure 7: Mass and width scan on $a_2(1670)$

There is a peak in the mass spectrum between 1.8 – 2.0 Gev. Because some theory predicts the lowest 1^{-+} exotic state is at about 1.9 Gev. So, we use a 1^{-+} to fit this region. Then we perform mass and width scan on this resonance. Unfortunately, the mass scan curve shows no minimum at this region. But if we use a 2^{++} or 0^{++} to scan this region, we could got quite beautiful scan curves which is shown in Fig. 9 – 10. So, our results favor a 2^{++} or a 0^{++} resonance at this region, and we could not find any strong evidence of the existence of a 1^{-+} resonance exists in this region. Structure here needs further study.

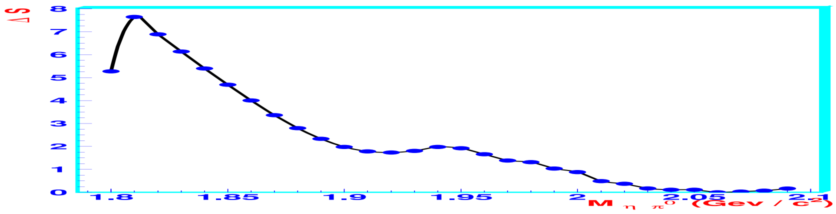

Figure 8: Scan 1.9 Gev region with a 1^{-+}

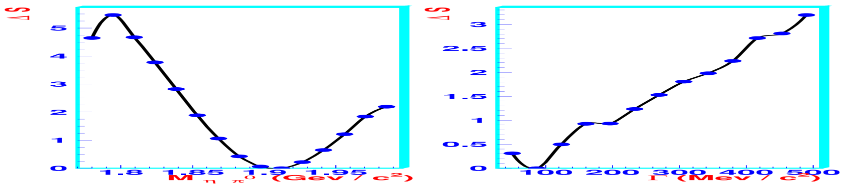

Figure 9: Mass and width scan on $a_0(1920)$

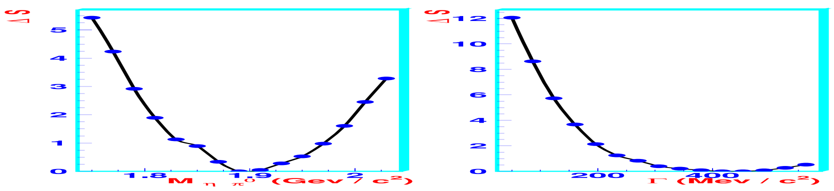

Figure 10: Mass and width scan on $a_2(1890)$

According to bin results, there are 4^{++} and 3^{-+} events at high mass region. We use all possible J^{PC} resonance to fit this region and then perform scan on it. And find that 1^{-+}, 3^{-+} and 4^{++} show clear dips at mass and width scan curves. Our scan results are shown in Fig. 11 – 13. These structures are also show in BESII data.

The mass and width of a resonance is determined from mass and width scan. Our results is listed in the Table II.

We also do another test on the J^{PC} of a resonance. That is, we try to see the change of the log likelihood when we change the J^{PC} of a resonance to some other values. The results are listed in Table III.

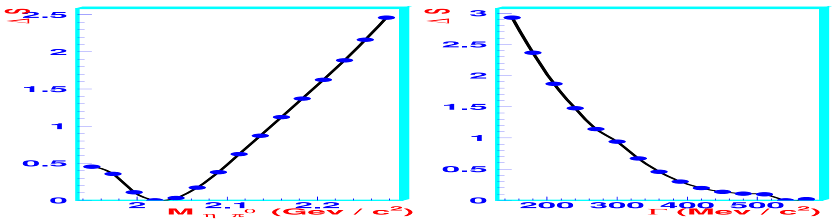

Figure 11: Scan 1.9 Gev region with a $a_4(2040)$

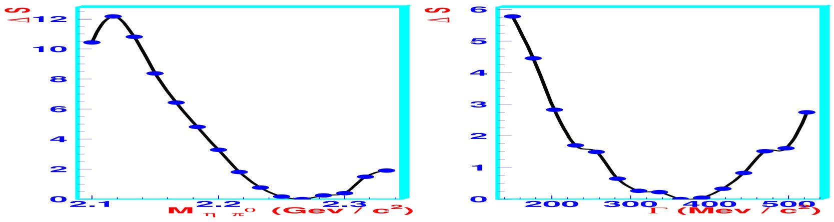

Figure 12: Mass and width scan on $\rho_1(2240)$

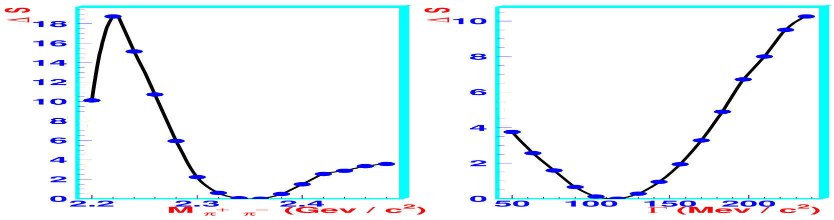

Figure 13: Mass and width scan on $\rho_3(2340)$

Resonance(J^{PC})	M(Gev)	Γ(Mev)	Effects	M_{pdg}	Γ_{pdg}
$a_2(1320)(2^{++})$	1325^{+50}_{-55}	130^{+122}_{-64}	5.13 σ	1.318	107
$\rho_1(1390)(1^{-+})$	1393^{+79}_{-60}	345^{+212}_{-150}	3.01 σ	1.370	385
$a_0(1450)(0^{++})$	1443^{+37}_{-53}	288^{+257}_{-123}	7.10 σ	1.474	265
$\rho_1(1590)(1^{-+})$	1582^{+117}_{-72}	300^{+401}_{-109}	1.90 σ	1.593	168^{+150}_{-12}
$a_2(1680)(2^{++})$	1683^{+68}_{-70}	150^{+171}_{-92}	2.96 σ	—	—
$\rho_1(2270)(1^{-+})$	2267^{+110}_{-59}	363^{+170}_{-163}	5.13 σ	—	—
$\rho_3(2300)(3^{-+})$	2360^{+110}_{-81}	117^{+59}_{-62}	6.11 σ	—	—

Table 2: Results on various resonance.

Resonance	0^{++}	1^{-+}	2^{++}	3^{-+}	4^{++}
$a_2(1900)$	1	7	—	10	25
$\rho_1(1390)$	17	—	10	8	20
$\rho_1(2270)$	6	—	17	7	34
$\rho_3(2300)$	9	11	13	—	9

Table 3: Test on J^{PC} of various resonance.

V. Summary

In this work, we use PWA method to study the invariant mass spectrum of $\eta\pi^0$. Some known resonances, such as $a_2(1320)$ and $a_0(1450)$, are found to be appear in this channel, and our results are quite close to those values which is given by PDG. Besides, we have found four resonances at 1390 Mev(1^{-+}), 1590 Mev(1^{-+}), 2270 Mev(1^{-+}) and 2300 Mev(3^{-+}) respectively. These results on mass and width are quite close to the values given by E852 experiment at BNL. It is possible to explain that they are exotic states, but need further confirmation and detailed analysis.

Besides, our analysis on $J/\psi \to \rho^{\pm}\eta\pi^{\mp}$ and $J/\psi \to \rho 3\pi$ is continuing. The invariant mass spectra of $\eta\pi^{\pm}$ and 3π are similar to that of $\eta\pi^0$. We expect the previous results can be confirmed in these channels.

Up to now, BESII has collected about 23M J/ψ events. We has also perform PWA analysis on the new BESII data and our preliminary results are quite close to the results that we have obtained in BESI data. The scan results on mass and width of some interested resonance is shown in table IV and our scan curve is shown in Fig. 14 — 17.

Resonance(J^{PC})	M(Gev)	Γ(Mev)	M_{BESI}	Γ_{BESI}	Effects
$a_2(1320)(2^{++})$	1310^{+15}_{-15}	140^{+30}_{-32}	1325^{+50}_{-55}	130^{+122}_{-64}	$\sim 11.5\sigma$
$\rho_1(1390)(1^{-+})$	1383^{+36}_{-33}	390^{+103}_{-92}	1393^{+79}_{-60}	345^{+212}_{-150}	$\sim 8.2\sigma$
$a_0(1450)(0^{++})$	1433^{+22}_{-28}	367^{+53}_{-74}	1443^{+37}_{-53}	288^{+257}_{-123}	
$\rho_1(1590)(1^{-+})$	1593^{+43}_{-25}	340^{+43}_{-81}	1582^{+117}_{-72}	300^{+401}_{-109}	$\sim 11.7\sigma$
$a_2(1680)(2^{++})$	1670^{+20}_{-23}	300^{+110}_{-52}	1683^{+68}_{-70}	150^{+171}_{-92}	$\sim 9.8\sigma$
$\rho_1(2270)(1^{-+})$	2270^{+27}_{-25}	420^{+80}_{-100}	2267^{+110}_{-59}	363^{+170}_{-163}	$\sim 13\sigma$
$\rho_3(2300)(3^{-+})$	2317^{+26}_{-31}	108^{+32}_{-22}	2360^{+110}_{-81}	117^{+59}_{-62}	$\sim 7.1\sigma$

Table 4: Results of BESII data.

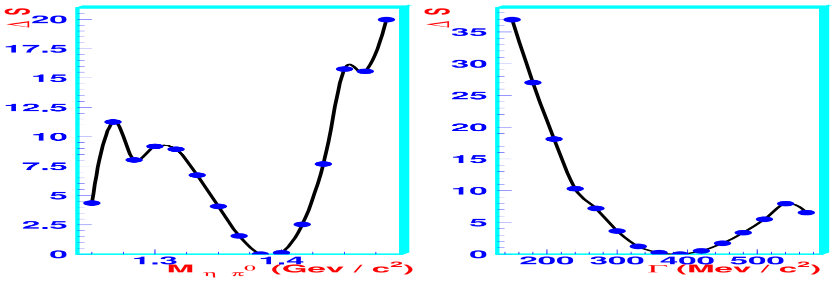

Figure 14: Mass and width scan on $\rho_1(1390)$ of BESII data.

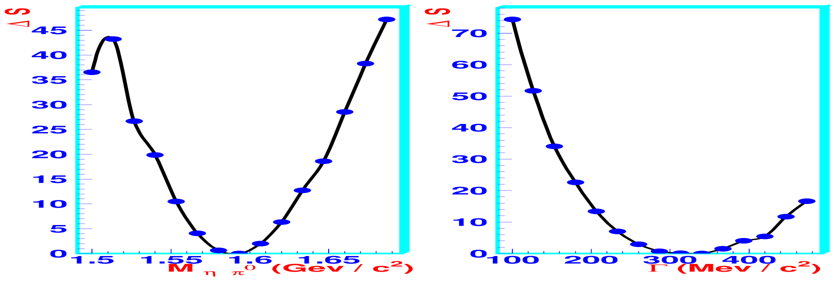

Figure 15: Mass and width scan on $\rho_1(1590)$ of BESII data.

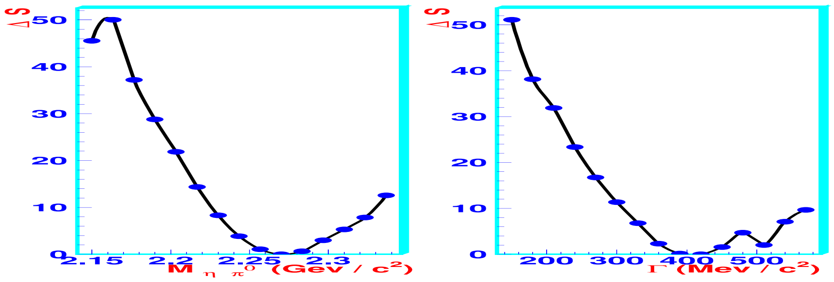

Figure 16: Mass and width scan on $\rho_1(2270)$ of BESII data.

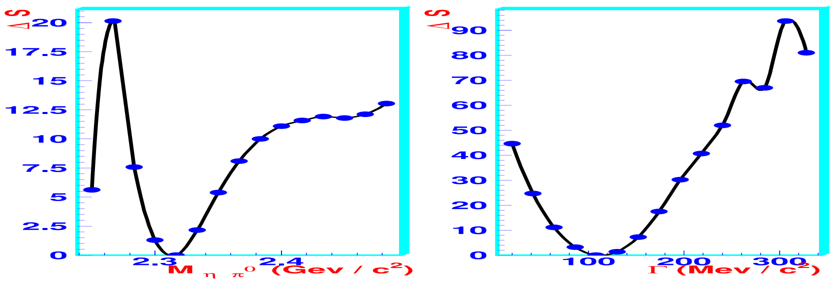

Figure 17: Mass and width scan on $\rho_3(2300)$ of BESII data.